

# Collaborative Pazy Wing Analyses for the Third Aeroelastic Prediction Workshop

Markus Ritter and Jonathan Hilger  
*DLR - Institute of Aeroelasticity*

André F. P. Ribeiro  
*Dassault Systems and Delft University of Technology*

Emre Öngüt  
*Siemens Digital Industries Software*

Marcello Righi  
*Zurich University of Applied Sciences ZHAW and Federal Institute of Technology Zurich ETHZ*

Cristina Riso  
*Georgia Institute of Technology*

Carlos E. S. Cesnik  
*University of Michigan, Ann Arbor*

Luiz G. P. dos Santos  
*University of São Paulo*

Daniella Raveh and Arik Drachinsky  
*Technion - Israel Institute of Technology*

Bret Stanford and Pawel Chwalowski  
*NASA Langley Research Center*

Ravi Kumar Kovvali and Beerinder Singh  
*Metacomp Technologies Inc.*

Stefanie Düssler, Kelvin Chi-Wing Cheng, and Rafael Palacios  
*Imperial College London*

João P. T. P. Santos, Flávio D. Marques Jr., and Guilherme R. Begnini  
*University of São Paulo and Federal University of Bahia*

Angelo A. Verri, João F. B. O. Lima, Felipe B. C. de Melo, and Flávio L. S. Bussamra  
*Instituto Tecnológico de Aeronáutica ITA and Embraer*

**In this paper, collaborative aeroelastic analyses of the *Pazy Wing* are presented, which support the activities of the *Large Deflection Working Group*, a sub-group of the 3<sup>rd</sup> *Aeroelastic Prediction Workshop* (AePW3). The *Pazy Wing* is a benchmark for the investigation of nonlinear aeroelastic effects at very large structural deflections. Tip deformations on the order of 50% semi-span were measured in wind tunnel tests at the *Technion - Israel Institute of Technology*. This feature renders the model highly attractive for the validation of numerical aeroelastic methods for geometrically nonlinear, large deflection analyses. A distinguishing feature of the *Pazy Wing* is that its flutter speed is a function of the static deformation, and capturing this effect requires a nonlinear aeroelastic framework which allows for stability (flutter) analyses about steady states of large deformations. In particular, the flutter characteristics of the model are dominated by a hump mode which develops due to the coupling of the first torsion and the second out-of-plane bending mode; this hump mode moves towards lower airspeeds as the steady structural deformation increases. Different nonlinear aeroelastic solvers were applied by the authors to obtain static coupling and flutter results for a series of airspeeds and angles of attack. The results reveal that the decisive nonlinear effects were captured very well by the applied methods and computational tools.**

## I. Motivation and Introduction

THE third Aeroelastic Prediction Workshop (AePW3) took place in conjunction with the 2023 AIAA SciTech Forum on January 21 and 22 in National Harbor, MD. The Large Deflection Working Group (LDWG) was one of the sub-groups of AePW3 and its purposes were, among others, to research the static and dynamic aeroelastic behavior of aircraft structures undergoing geometrically large deformations and to gain deeper understanding of the physical mechanisms involved. It was also desired to understand which particular features an aeroelastic solver requires for the comprehensive analysis of aircraft structures with geometrical nonlinearities. This particular objective was sparked by the emerging trend in the aircraft industry towards slender, high aspect ratio wings (with increased flexibility), motivated and forced by the need to massively increase energy efficiency by reducing drag. The structural flexibility of aircraft or aircraft components investigated by aeronautical researchers was thus increased continuously. Terms such as "large deflections", or "highly flexible aircraft" appeared to emphasize the flexibility of the systems; however, such definitions are not precisely defined and are often used to describe aeroelastic structures whose properties indeed are characterized by the (possibly large) flexibility of the structure, but do not necessarily experience particular (geometric) nonlinearities in normal operation. The decisive factor is that in order to accurately predict the aeroelastic behavior of *true* "highly/very flexible aircraft", (geometrically) nonlinear aeroelastic tools with both nonlinear aerodynamic and structural methods are indispensable – or by other words, the application of linear aeroelastic simulation programs would yield inaccurate or erroneous results. The certification of that statement was one of the goals of the activities of the LDWG.

Nonlinear aeroelastic simulations call for computational frameworks that can model (geometrical) nonlinearities, this significantly increases the complexity for the implementation. Besides that, verification and validation of such tools are indispensable and require suitable data from other numerical methods or, preferably, from experiments. In past years, aeroelastic experiments indeed were focused towards more flexible wings to gain better understanding of the physical mechanisms involved and to provide validation data, but comprehensive and publicly available experimental data sets of highly flexible test cases are scarce [1–3]. At the beginning of the activities of the LDWG in 2019, various test cases were proposed by several research institutes. However, only very few were suitable for the LDWG. Essential criteria, such as freely available and detailed experimental data and simulation models or the extent of nonlinearities had to be fulfilled. Finally, a decision on the test case was made in favor of the Pazy Wing, a highly flexible wind tunnel model with remarkable nonlinear aeroelastic characteristics [4–6]. This wing was specifically designed to provide freely available experimental data to the aeroelastic community that can be used for the validation of numerical methods in the nonlinear regime with large deflections.

As a motivating example to highlight the unique nonlinear features of wings (and in particular of the Pazy Wing) in very large deformations, three physical phenomena that are rarely found on other flexible (or even very flexible) aeroelastic test cases are depicted in Fig 1. The first nonlinear effect is a simple geometric one that intensifies with increasing structural deformations: finite elements and structural nodes move along curved paths rather than straight lines (as in a linear approach). Considering an aeroelastic system, this leads to in-plane components of the aerodynamic forces – they are nonconservative in nature; furthermore, the current/instantaneous location of nodes must be employed, e.g. for the calculation of loads along the wing to account for correct lever arms. The second effect is the dependence of the structural eigenvalues (mode shape frequencies) on the deformation. In the undeformed/jig state, out-of-plane and in-plane bending as well as torsion modes are decoupled and distinguishable, but they become coupled with increasing levels of deformation. Finally, these two effects manifest in a strong dependence of the dynamic stability of the wing on the static deformation (or likewise, on the combination of the root angle of attack of the wing and the airspeed).

This paper gives an overview of the collaborative activities of the LDWG – the investigation and modeling of the highly nonlinear aeroelastic behavior of the Pazy Wing. Following the introduction of the Pazy Wing test case, the aeroelastic simulation methods of the authors are described and the results are compared with experimental data provided by Technion. The activities involve static coupling simulations for three different angles of attack (three degrees, five degrees, and seven degrees) and a range of dynamic pressures (up to 2400 Pa, which corresponds to an airspeed of approximately 62 m/s for sea level conditions), computation of the frequencies of the lowest five structural mode shapes as function of the static deformation of the wing, as well as the computation of the flutter on and offset speeds for the first instability region, which is a hump mode that migrates depending on the static deformation. Aeroelastic simulations from the authors are all based on geometrically nonlinear structural methods – which are indispensable for this test case – coupled with potential aerodynamics, such as strip theory, steady and unsteady vortex-lattice methods (VLM and UVLM), doublet-lattice method (DLM), 3D source and doublet panel method, and a CFD-based framework. As the focus of this work is the comparison of static coupling deflections and flutter speeds where the aerodynamic forces mostly show linear dependence on the local angle of attack, nonlinearities due to viscous

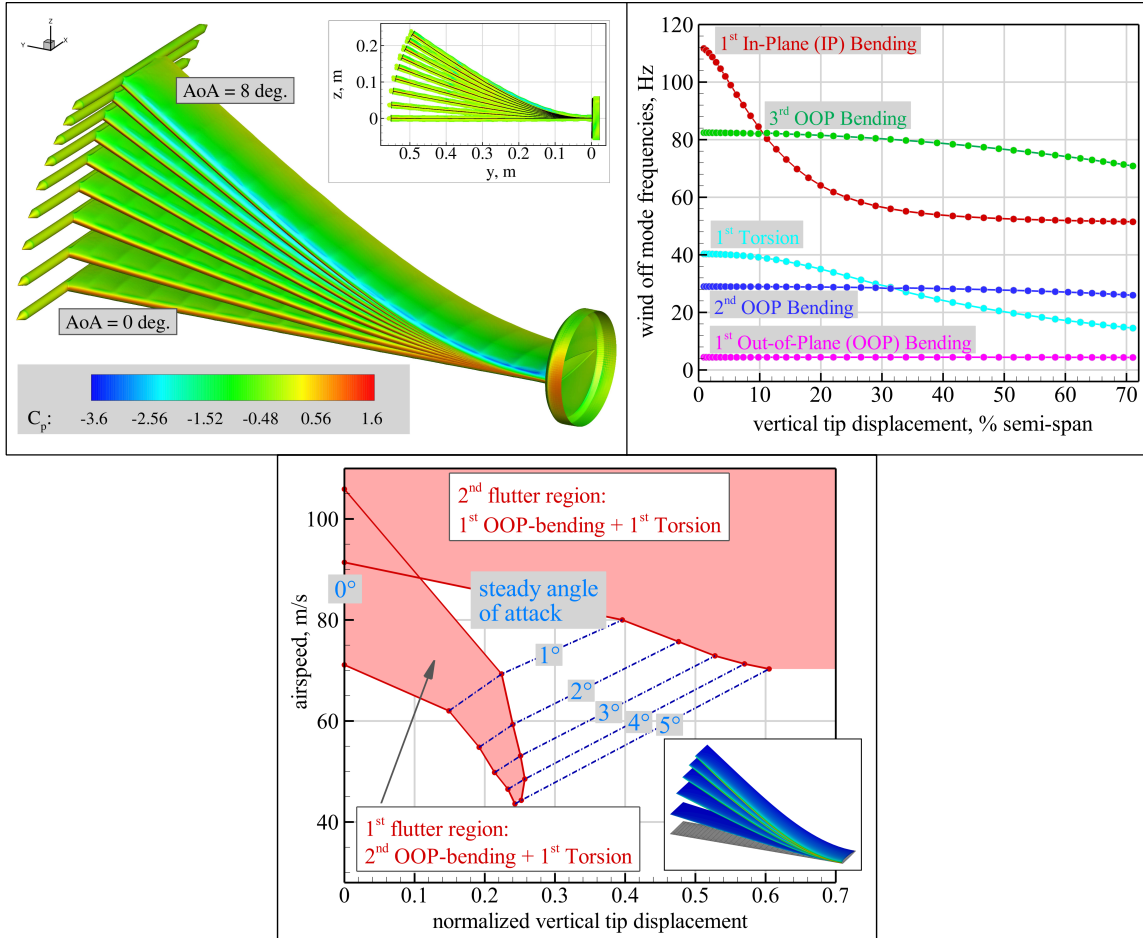


**Fig. 1 Three distinctive, nonlinear aeroelastic effects of a wing undergoing very large deformations. Geometrically nonlinear displacement fields with pronounced in-plane components of the aerodynamic forces (upper left plot). Structural eigenvalues are a function of structural deformations (upper right plot). Dependence of the dynamic stability of the wing on the static deformation (lower plot), which combines the upper two effects.**

effects (stall) and thickness can be omitted. The AePW3 web page provides a good overview of the activities of the LDWG <sup>§</sup>, and detailed information about the individual simulation activities are given in recent publications [5–21].

## II. The Pazy Wing Benchmark Model

In this section the Pazy Wing is described with a focus on its main geometric, design, and manufacturing features. Also the simulation models (CAD and structural models), which were provided for the LDWG, are introduced briefly. More details about the design, manufacturing, static and dynamic structural, as well as wind tunnel testing are given in the publications from Technion [4, 5]. Only those key aspects that are relevant regarding the aeroelastic simulations and validations are repeated in the following subsection.

### A. General Features

The Pazy Wing was designed as a benchmark model at the Technion to study aeroelastic phenomena associated with geometrically nonlinear, very large deflections [4]. Although aeroelastic systems with geometrically nonlinear, large deformations have been investigated theoretically for a longer period, only very few experiments with focus on wings or aircraft subject to large, nonlinear deformations have been presented over the past decades. The Pazy Wing

<sup>§</sup><https://nescacademy.nasa.gov/workshops/AePW3/public>

is a one-of-a-kind benchmark, which was tested deep in the nonlinear regime. As demonstrated in the following sections, the application of linear aeroelastic tools yields incorrect results, thus it can be considered a *true very flexible aeroelastic system*. The Pazy Wing wind tunnel model from Technion is shown in Figure 2. Unique features make this

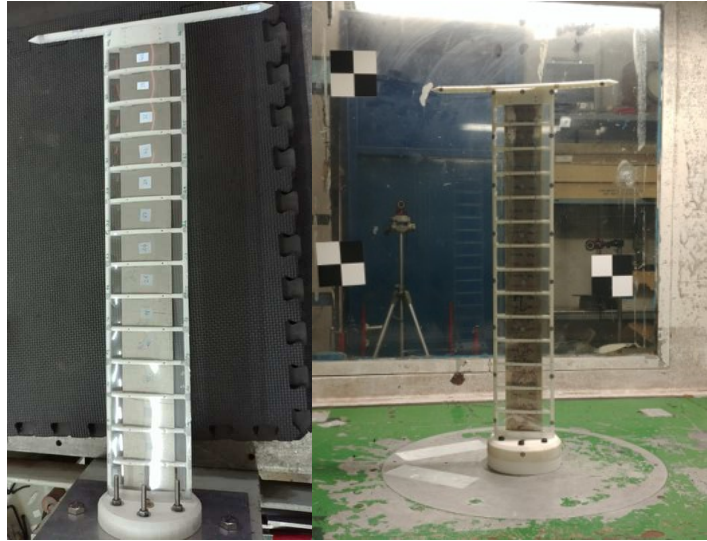


**Fig. 2 Pazy Wing in the laboratory and in the wind tunnel at Technion - Israel Institute of Technology.**

test case interesting for a broad audience. The geometry and the test conditions of the model are simple: a wing with rectangular planform, no taper, no sweep, and a symmetrical airfoil (NACA 0018) that operates in an incompressible flow regime (the Mach number is approximately 0.15 for the highest airspeed in the wind tunnel tests). The main dimensions and selected details of the model are listed in Table 1.

**Table 1 Dimensions and details of the Pazy Wing wind tunnel model.**

Property	Unit	Pazy Wing
Semi-span	m	0.55
Chord (without tip rod)	m	0.1
Reference surface (without tip rod)	m <sup>2</sup>	0.055
Clamping section height	m	0.021
Clamping section diameter	m	0.12
Tip rod length	m	0.3
Tip rod diameter	m	0.01
Airfoil	-	NACA 0018
Chassis / Rib structure	-	Nylon (Polyamide 12), 3D printed
Covering	-	Oralight (polyester shrink film, 12 $\mu$ m) *

## B. Models for the Aeroelastic Simulations

As mentioned above, the simulation models and experimental data of the Pazy Wing test cases investigated by the LDWG are freely available. These include, amongst others, a CAD model, a full FEM (with the clamping section, the spar, the ribs/chassis, and the foil covering modeled in detail by beam, shell, and solid finite elements with specific material properties). An aeroelastic simulation model comprises of an aerodynamic and a structural model, both of course depend on the particular numerical simulation program that is applied. The aerodynamic model can be setup

\*<https://www.oracover.de>

based on the CAD model where for aerodynamic methods based on potential theory only the edge points and the symmetric NACA 0018 airfoil section (if thickness effects are to be considered) are required. For CFD aerodynamics, the outer geometry including the cylindrical clamping section and the tip rod is available as CAD (IGES), both as a "clean wing" without the sagging between the ribs (as it comes from the CAD model) but also in the form of a "real wing" including the sagging between the ribs and the small discontinuities in the surface that come from the foil covered Nylon chassis <sup>†</sup>. A screenshot of the original CAD model, the full FEM (for use with Nastran), and the outer surface of the Delft University of Technology Pazy Wing (from a 3D scan) are displayed in Figure 3. Because of the small

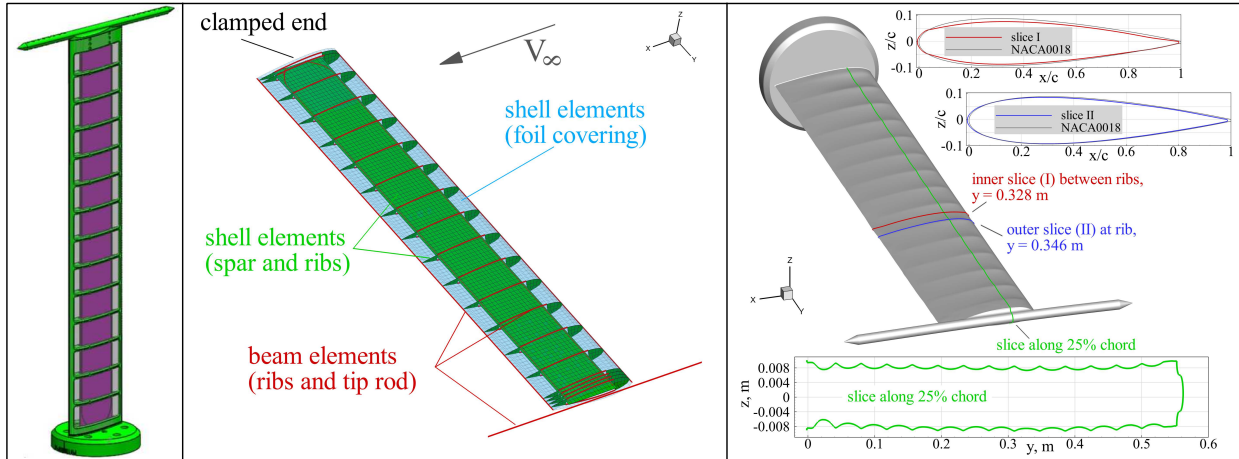


**Fig. 3 CAD sketch, full FEM, and outer surface of the Pazy Wing. The outer surface plot (on the right) corresponds to the TU Delft Pazy Wing [22].**

dimensions of the Pazy Wing in comparison to the Technion wind tunnel dimensions (as it can be seen in Figure 2), the inclusion of the wind tunnel walls in the aerodynamic model seems unnecessary and a symmetry boundary condition at the root is appropriate.

The structural model is provided both as a full FEM and in the form of (beam) cross section data along the span [8, 9] <sup>‡</sup>. A beam model is a convenient, general structural approximation, because the beam cross section data (stiffness and mass properties) can be used for all types of (geometrically nonlinear) beam models – including commercial FE tools such as ANSYS or Nastran. It should be mentioned that the structural properties, such as the bending stiffness in two directions, the torsion stiffness, and the mass distribution are almost constant along the span of the wing due to constant cross section of the aluminum spar and the Nylon chassis. As mentioned above, the full FEM is much more detailed but a problem arises with its application in a nonlinear FE solution (e.g. Nastran SOL 400). The foil covering – modeled by shell elements – adds a small but significant stiffness to the structure, but these elements tend to buckle even at low deformations on the compressed side of the wing if the pre-tension (due to the shrink from the manufacturing process) is not accounted for. So far, no simple solution has been found in the LDWG to solve this problem, thus the (nonlinear) beam model is at present the preferred solution for the structural part. The lowest five mode shapes of the undeformed structural model, which play a decisive role in the aeroelastic analyses (as will be highlighted in the following sections), are plotted in Figure 4.

### III. Individual Aeroelastic Simulation Models and Computational Frameworks

In this section, individual approaches, methods, and simulation frameworks applied by the authors are described. As mentioned in the previous sections, an essential capability of the applied method is the modeling of nonlinearities in both the aerodynamic and the structural disciplines (depending on the particular method for the numerical discretization, a nonlinear approach for the fluid-structure coupling process might become necessary as well). A number of papers have been published by members of the LDWG over the past years in which their specific simulation activities, methods and results are detailed. The corresponding references are listed with the individual description of the activities.

<sup>†</sup>Another Pazy Wing, which was built by Delft University of Technology based on the CAD models from Technion, was 3D scanned and the geometry was processed by NASA to create an IGES file suitable for CFD grid generation. This geometry is freely available from the authors [17, 22].

<sup>‡</sup><https://github.com/UM-A2SRL/AePW3-LDWG.git>



**Fig. 4** Lowest five natural mode shapes as computed by MSC Nastran of the undeformed Pazy Wing full FEM with skin (OOP = Out-of-Plane bending, T = Torsion, IP = In-Plane bending).

### University of Michigan and Georgia Tech

The Pazy wing analyses by the University of Michigan and Georgia Tech team leveraged the University of Michigan’s Nonlinear Aeroelastic Simulation Toolbox (UM/NAST) [23]. UM/NAST is a multidisciplinary framework for modeling, analyzing, and simulating very flexible wings and complete aircraft while capturing coupling effects among structural dynamics, rigid-body dynamics, and aerodynamics. The framework models each aircraft’s structural component (e.g., wing) as a non-isotropic beam undergoing arbitrary deflections relative to a body-fixed frame, which is in rigid-body motion within an inertial frame. Elastic deflections are modeled using the geometrically exact, strain-based beam formulation of Su and Cesnik [24], which assumes four strain DOFs per beam element: axial extension, twist, and out-of-plane and in-plane bending curvatures. Shear effects are condensed through energy minimization [25], leading to a  $4 \times 4$  cross-sectional constitutive law between the axial, torsion, and bending strain measures and the cross-sectional stress resultants (axial force, twisting moment, and bending moments, respectively). Once the model strain vector is known, the deformed shape is recovered by marching the kinematic relations in space [23, 24]. This strain-based formulation can be coupled with various steady and unsteady aerodynamic models available in UM/NAST, ranging from airfoil theories to Kriging surrogates and UVM. The resulting aeroelastic equations are further coupled with rigid-body dynamics equations for free-flight analyses and simulations of complete aircraft. The framework also has numerical linearization capabilities to enable aeroelastic eigenvalue analyses, which were used to predict the flutter characteristics of the Pazy Wing. Additional details on UM/NAST are given in Refs. [23, 24].

The Pazy Wing structural model in UM/NAST consists of equivalent beam inertia and stiffness properties along a reference axis at 44% chord. These properties were extracted in Ref. [8] from a variant of Technion’s built-up FEM [4] with a rigid tip rod using the University of Michigan’s Enhanced FEM2Stick (UM/EF2S) framework [26]. The aerodynamic model consists of the unsteady potential flow thin airfoil theory of Peters et al. [27] with user-specified cross-sectional aerodynamic coefficient derivatives. Two aerodynamic model variants are available, one that assumes a flat-plate airfoil and captures wingtip effects using tip loss corrections [8], and a second one that uses spanwise variable aerodynamic coefficient derivatives [9] provided in [5]. All the UM/NAST results in this paper are based on the first aerodynamic model [8] except for the natural frequencies in the aeroelastic deformed shape, which are based on the second one [9]. Additional details on the Pazy wing UM/NAST models are given in Refs. [8, 9]. The model properties are publicly available for download from the authors’ GitHub repository<sup>§</sup> along with the UM/NAST results. Higher-order models of the Pazy wing were also analyzed in Nastran solvers for verification and model fidelity studies [8, 9]. These models consist of the built-up FEM variant with a rigid tip rod coupled with VLM and DLM models for static and dynamic aeroelastic computations.

### Technion

The Pazy wing simulations were performed with the Modal Rotation Method (MRM), a modal-based nonlinear framework for static and dynamic aeroelastic solutions of very flexible configurations that undergo large deformations [5, 28]. The MRM uses the structure’s linear modes, which can be computed via a linear FE-based free vibration analysis or a modal test. The MRM is suitable for wing geometries that are beam-like. I.e., geometries that have a long span dimension compared with the other two dimensions. The FE-computed displacement modes are transferred (interpolated) into a reference line along the span direction and are used to compute the incremental rotation modes of segments over the reference line. These rotation modes are used in the analyses, rather than the displacement modes.

<sup>§</sup><https://github.com/UM-A2SRL/AePW3-LDWG.git>

The reference line can be partitioned into many segments, thus ensuring that the incremental rotation at each segment is small even in cases of large wing deformations. Thus, the rotation modes can be used in linear analysis and the overall incremental rotation of each segment can be computed as a linear sum of the rotation modes. To compute the static displacements, segments are sequentially rotated into their place in a global coordinate system. The MRM employs a moment correction method to correctly account for the locations and orientations of the external loads [28]. The Pazy wing static aeroelastic analysis was performed with strip-theory aerodynamics, obtained from a DLM model and corrected for finite wing and wing-tip effects [5].

For the aeroelastic dynamic flutter analysis, the rotation modes are projected onto the statically deformed geometry and the generalized mass and generalized aerodynamic force coefficient matrices are updated to account for the deformed-shape modes [5]. The linear aerodynamic force coefficient matrices are computed in the ZAERO aeroelastic software based on linear DLM.

The MRM can be used in either a direct approach, which uses the discrete mass distribution along the reference line, or a fully-modal approach, which only requires information on the modes and generalized matrices of the linear, undeformed geometry. The latter can be used with complex FE models and does not require reducing the model to an equivalent beam, thus saving significant pre-processing efforts. The MRM was also used to estimate the Pazy wing's dynamic response in the flutter test based on strain data measured in optical fibers [7].

### **Imperial College London**

SHARPy [29] is an open-source, nonlinear aeroelastic simulation environment for simulation analysis and control system design. An outline of the workflow and modules necessary for computing flutter in highly flexible, clamped wings over a wide range of test parameters is summarized next and for a more detailed description, the reader is referred to [11]. SHARPy's main components are a displacement-based, geometrically-exact composite beam model (GEBM) for the structural dynamics and an UVLM for aerodynamics. Both the GEBM and UVLM are strongly coupled for fluid-structure interaction (FSI) problems. With this solver, we compute the deformed state of our aeroelastic model, linearize the system, and reduce the obtained nonlinear aeroelastic equilibrium. The linearization is performed for the UVLM and GEBM independently [10]. The UVLM linearization is performed analytically, assuming constant AICs and a frozen wake shape while including steady load effects. The resulting discrete linear time-invariant (DLTI) system is then efficiently reduced using Krylov subspace methods [30]. Next, the GEBM is linearized around the same reference equilibrium condition and further reduced by projecting it onto the modal coordinates of the deformed system. This system can be truncated to a suitable number of modes that capture the most important dynamics for the given system and is then coupled with the reduced aerodynamic system. The eigenvalues are finally computed for the resulting aeroelastic system and the resulting damping and frequency characteristics are extracted from which the flutter speeds can be obtained. We use two approaches to find these flutter speed solutions:

- 1) We assume a frozen geometry at one specified nonlinear aeroelastic equilibrium, defined by a free stream velocity  $U_\infty$  and root angle of attack  $\alpha$  for the Pazy Wing. We then consider a range of free stream velocities to determine the flutter margin for the linearized system obtained at this particular equilibrium point.
- 2) For each equilibrium point (defined again by  $U_\infty$  and  $\alpha$ ), the eigenvalues of their linearized systems are computed and stability is assessed. This determines the stability boundary of the geometrically nonlinear wing.

### **DLR**

The aeroelastic simulations of DLR are based on a steady and unsteady as well as a linearized vortex-lattice method (UVLM). The implementation uses vortex rings for the bound and wake panels with equal and constant circulation of the four vortex filaments (zeroth order formulation) [31, 32]. The wake can be relaxed (although this option was not used for the Pazy Wing simulations) and the aerodynamic panels can undergo almost arbitrary deformations and rotations. The computational grid is updated at each deformation increment (or timestep for time-domain simulations) and the aerodynamic forces are calculated using the actual geometry of the wing/panels [3, 15, 33]. Induced drag is calculated from induced velocities, viscous drag is estimated based on local Reynolds numbers and airfoil polars pre-computed by XFOIL [34]. For the static coupling simulations, the structure was solved by MSC Nastran nonlinear solution sequence *SOL 400* and also the mode shapes with corresponding frequencies (both for the undeformed and the deformed configuration) were calculated by this method [35]. For the aeroelastic stability (flutter) analyses of the Pazy Wing, a state-space model is built by linearizing the entire aeroelastic system about a particular steady (equilibrium) state of the static coupling simulations. The linearization approach and process is described in detail in the publications of Hilger and Ritter [14, 36]. The poles of the linear state-space system indicate the stability of the system.

DLR uses the beam model provided by University of Michigan and NASA for all simulations [8, 9]. It was "extended" to a 3D-like model (referred to as "couplingmodel") by adding structural nodes at the leading and trailing edges along the span, which are connected to the beam nodes by massless, rigid bars (Nastran RBE2 elements) [15, 16]. DLR also applied a CFD-based approach to simulate polars of the rigid Pazy Wing for a range of root angles of attack and dynamic pressures. Therefore, both a "clean wing" without rib sagging and the real shape (of the Delft University of Technology Pazy Wing) including the sagging between the ribs were used. The focus of these simulations were the investigation of the impact of free transition modeling and the undulated rib structure mainly on the aerodynamics [16, 22]. Further simulations will be conducted in which the CFD approach is used for time-domain simulations of limit cycle oscillations of the Pazy Wing. For the comparisons within this paper, only the UVLM results of the DLR simulations are considered.

## NASA

Static aeroelastic analysis is conducted by coupling a linear aerodynamic panel tool (DLM) to a nonlinear beam solver. Both the aerodynamic and structural solvers are found in MSC Nastran, but Nastran's internal aeroelastic solvers can only compute linear mechanisms, and a nonlinear interaction (via the structural beam) is considered here. Therefore, a Matlab tool is written to externally couple the Nastran DLM to the Nastran nonlinear beam solver, iterating between the two until convergence is obtained at a specified dynamic pressure  $q_\infty$  and root angle of attack. Once this static aeroelastic process has converged, Nastran is used to compute the natural vibration frequencies and mode shapes about the statically deformed beam.

Next, a dynamic aeroelastic analysis is conducted via frequency domain aerodynamics, again using the DLM inside Nastran. The mode shapes are interpolated onto a DLM mesh which has been deformed to match the static aeroelastic shape, and the generalized aerodynamic forces (GAFs) are computed at a range of reduced frequencies ( $k$ ). These GAFs are a three-dimensional matrix, of size  $N_{modes} \times N_{modes} \times N_k$ . The GAFs are only valid for a single dynamic pressure: changing the dynamic pressure will change the static aeroelastic deflection, changing the modal content (this is in contrast to linear aeroelasticity, where the GAFs are independent of  $q_\infty$ ). Since flutter computations (via the  $p - k$  method, in this work) are done by sweeping across  $q_\infty$ , we must also compute GAFs across a range of pre-selected  $q_\infty$  values, and linearly interpolate as needed. A specialized  $p - k$  method has been written which can handle this nonlinear dependence of GAF upon  $q_\infty$ . The flutter point is finally computed as the  $q_\infty$  at which an aeroelastic mode travels into the right-half of the complex plane [17].

## Metacomp Technologies Inc.

All results submitted were obtained using Metacomp's suite of software products. CFD++, a comprehensive, general purpose fluid dynamics solver, was used to run a CFD simulation on an unstructured 7.2 million cell mesh (containing tetrahedrals, hexahedrals, pyramids and triangular prisms). The compressible Navier-Stokes equations (calorically perfect gas) were solved using a preconditioning algorithm for this low speed flow. Turbulence closure in these URANS simulations were obtained using a realizable k-epsilon turbulence model. For the structural solver, we used CSM++, a nonlinear 3D finite element solver that is able to import and work with the Nastran model of the Pazy wing (without the skin and the 10g trailing edge mass) provided by Technion. Both codes were used in a partitioned manner and coupled using MetaFSI. Pressures and wall shear data from the CFD boundaries are transferred to the appropriate boundaries on the FE mesh as forces and moments by MetaFSI. Once the structural deformations are computed, MetaFSI is also responsible for transferring these deformations back to the CFD boundaries and then morph the rest of the CFD volume mesh by building radial basis function (RBF) based interpolants. The coupling type between the codes is implicit — both codes exchange loads and deformations back and forth during each time step to converge within a given tolerance before proceeding to the next physical time step. All results presented use a time step of 0.0001 s. Internally, simulations with different time-steps were conducted and 0.0001 s was deemed satisfactory from a convergence perspective. More information regarding CFD++, CSM++ and MetaFSI can be found at the web page of Metacomp Technologies <sup>¶</sup>.

## ITA and Embraer

The team ITA-Embraer has used a simplified methodology to predict the onset and offset flutter velocities of very flexible wings. First, the static aeroelastic computation is conducted by loosely coupling the implicit nonlinear

---

<sup>¶</sup><https://www.metacomptech.com>



structural solver to a full potential aerodynamic solver with a boundary layer correction. Subsequently, a flutter solution is computed about the deformed geometry. The proposed framework outputs frequency and damping diagrams in matched state, where every flight speed is related to a deformed wing shape with its flutter solution. This method is able to obtain a match within 5% difference to the experimental data, by simply deforming the aerodynamic and structural mesh of the Pazy Wing using a framework to interface with commercially available solvers [18, 19, 37, 38].

## **SIEMENS**

Siemens employed a methodology based on off-the-shelf industrial solvers for linear aeroelasticity and nonlinear structures. This methodology loosely couples the linear aeroelastic solver Simcenter Nastran SOL 144/5 and the nonlinear structural solver Simcenter Nastran SOL 402 and is similar to the approaches investigated previously by others, such as Zhao et al. [39] for the SUGAR truss-braced wing, and Xie et al. [40]. For the static solution, the effect of wing twist on the aerodynamics is captured by extracting the twist information from the nonlinear structural solution and applying it in Nastran aeroelastic analyses with DMI W2GJ cards [41]. Similarly, the follower effect of the aerodynamic loads is captured by applying them to the nonlinear model as follower forces using Nastran FORCE2 cards. This coupled process is automated with an NX Open Python script to reach a converged static response for the given dynamic pressure and angle of attack.

Subsequently, the static workflow is extended to determine the flutter onset boundary. The process starts with an initial estimation of the flutter speed and the static nonlinear analysis process explained before is executed for this operating condition. After the converged nonlinear static response is obtained, the pre-stressed modes are extracted from the results of the nonlinear structural analysis and imported to SOL 145. This effectively linearizes the structural model, taking into consideration the effect of geometric stiffening under highly deformed conditions. The Simcenter 3D user interface is used to import the pre-stressed models in Simcenter Nastran SOL 145 and no DMAP routine is needed. The initial estimation of the flutter speed is varied until the estimate and the flutter speed obtained from SOL 145 match.

## **SIMULIA and Delft University of Technology**

Simulations conducted by Ribeiro et al. [20, 21] employ a free wake panel method coupled to a geometrically exact beam model. Simulations are conducted in the time domain. A source and doublet panel method formulation is used, which model the entire wing surface. Wake panels with are created every timestep, enforcing the Kutta condition at the trailing edges. Sources ensure impermeability, while doublets are solved for by a linear system of equations using the influence coefficient matrices for the doublets, sources, and wake vortices. The system of equations corresponds to the different contributions to the flow potential on the center a surface panel, where there are contributions from all surface panels and all wake panels. The values of sources, doublets, and wake vortices are constant over each panel. At every timestep, wake vortices are convected due to the freestream velocity and the induction of all the surface and wake panels. The surface velocity can be taken from the gradient of the potential, which is computed with central differences for quadrilateral panels, and a least squares approximation for triangular panels. With the surface velocity available, the unsteady Bernoulli equation is used to find the surface pressure, which is then used to compute the forces on the structural model.

The structural deformation of the wing is computed with a geometrically exact beam model. This allows for nonlinear, time-domain calculations with large deflections, anisotropic deformation couplings, and curved beams. The structural properties of the beam model are imposed with a Timoshenko stiffness matrix and a mass matrix, both provided by the University of Michigan and created with UM/EF2S. A loosely-coupled approach for the aerodynamics and structural solvers is used to allow for fluid-structure interaction simulations. The coupling methods consist of a nearest-neighbor method for converting the aerodynamic loads to the structural model, including forces and torques of each surface panel, and an orthogonal projection spline approach to convert the structural displacements to the aerodynamic panels. Although the nearest-neighbor method does not conserve virtual work, the associated error for the Pazy Wing simulations was measured and stayed below 2%, which was considered satisfactory. The influence coefficients are recomputed at every timestep, to account for relative motion between the panels. The main nonlinear effects that the current implementation neglects are related to flow separations, as the aerodynamic model is inviscid and hence unable to capture static or dynamic stall.

The Pazy Wing was modeled using quadrilateral panels, with 150 panels in the chordwise direction with a cosine distribution (refining the leading and trailing edges), and 26 panels in the spanwise direction, with a uniform distribution. A symmetry plane is placed on the wing root to model the wind tunnel wall, mirroring the wing surface and wake

panels by using virtual panels. The timestep is set to  $\Delta t = 0.25c/U_\infty$ . Resolution studies were performed for the surface mesh and timestep lengths. Wake panels are deleted once they reach the arbitrary location of  $x = 10s$  (where  $s$  denotes the span of the wing), as this saves computational time and does not affect the results noticeably. Simulations are conducted for at least 2000 timesteps, or 500 flow passes, where the first 4 timesteps are used to initialize the wake, with a rigid wing. Further details on the methods and results can be found in the article of Ribeiro [21].

#### **University of São Paulo and Federal University of Bahia**

The influence of a nonlinear static deformation on the dynamic aeroelastic behavior of very flexible wings, here the Pre-Pazy and Pazy Wings, is analyzed. A time-domain aeroelastic model capable of predicting the flutter behavior of these wings is developed. For the structural part, the FEM is applied and the structure is discretized in nonlinear beam elements, which are formulated in terms of the nonlinear von Kármán strains [42, 43]. The VLM and UVLM are considered for aerodynamic modeling [31]. To predict the flutter of the wing, a nonlinear static aeroelastic coupling analysis is performed first, coupling the nonlinear beam formulation with the VLM, for a set of root angles of attacks and flow speeds. The Newton-Raphson (NR) method is applied to find the static equilibrium of the structure. The stiffness matrix of the deformed structure is applied in a modal analysis to compute the natural frequencies and mode shapes of the pre-deformed structure. These data serve as input for the dynamic aeroelastic model, which uses the UVLM as aerodynamic model. The structural and aerodynamics model are coupled together by means of a surface spline interpolation method, and a predictor-corrector method is applied to solve the equation of motion iteratively on a time-domain basis [44]. As output data, the time responses of the wing in modal coordinates are obtained. For an effective prediction of the flutter, the modal parameters, more specifically frequencies and damping ratios, must be determined. The frequency spectrum of each time response serves as input for a modal parameter identification method, which uses the Least Squares Complex Frequency-domain estimator (LSCF) [45]. From the modal parameters identified, the velocity-damping-frequency (V-g-f) diagrams are obtained and the flutter speeds and frequencies are determined for a set of root angles of attack [46, 47].

#### **University of São Paulo, USP/DAB-Framework**

The University of Sao Paulo’s Dynamic and Aeroelasticity of Beams (USP/DAB) is a simulation tool that employs a 1-D beam finite-element implementation of the mixed-formulation of the geometrically-exact theory of beams. In it, the elemental DOFs are displacements, rotations, internal forces and moments, as well as linear and angular velocities. Each element is assumed to have an aerodynamic strip attached to it. The structural model is coupled to a semi-empirical dynamic stall model, which is capable of capturing nonlinear aerodynamic phenomena due to high angles of attack, and whose linear part is computed with an indicial application of the thin-airfoil theory. For the Pazy Wing simulations, 3D aerodynamic effects are captured by the VLM-fitted span correction function devised by Riso [48], which corrects the 2-D aerodynamic coefficients given by the strip theory. The airfoil of the wing is assumed to have a lift-curve slope of  $2\pi/rad$ , and all other relevant steady aerodynamics properties are zero. There are currently no publications that could be used as reference for the present methodology and its results, but a related PhD dissertation (Luiz G. P. dos Santos) is ongoing.

## **IV. Static Coupling Simulations and Comparison to Experimental Data**

The first aeroelastic analyses of the Pazy Wing is the static coupling simulations. The goal of this activity is to demonstrate that each individual aeroelastic simulation model and framework is able to capture the nonlinearities which emerge both in the structural and in the aerodynamic discipline as mentioned in the introduction. Tip displacements up to 50% with respect to the semi-span of the wing illustrate in particular the high degree of nonlinearity involved.

### **A. Experimental Data of the Steady Wind Tunnel Tests**

In the experimental wind tunnel tests, the model was mounted vertically on a turntable that allows for adjusting the root angle of attack, as it can be seen in Figure 2. A balance was mounted between the wing and the turntable to measure the loading of the wing. The dynamic pressure was changed from 50 to 1800 Pa by increasing the airspeed in the tunnel. Experimental data in terms of loads at the wing root and deformations (measured optically and by strain gauges) are available for three, five, and seven degrees angle of attack. Detailed information about the wind tunnel tests of the Pazy Wing are given in the publications of Technion [4–6]. In the following, we focus on the comparison of the static elastic deformation of the wing at its tip (at mid-chord) in the vertical direction as predicted by the static

coupling simulations with the corresponding experimental data. We consider this as the most interesting quantity for the activities of the LDWG. Comparisons of other quantities are partly presented by individual publications of the research groups.

Figure 5 shows the wingtip displacements at mid-chord for varying dynamic pressure and three different root angles of attack. This data will be used for the following comparisons with the simulation results. The kinks and irregularities

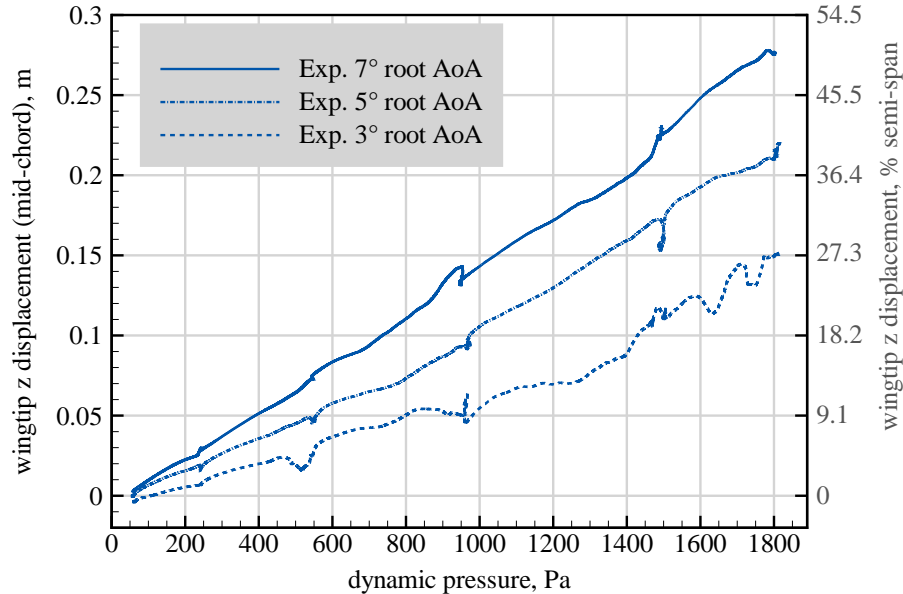


**Fig. 5 Wingtip displacements (at mid-chord) as a function of the root angle of attack and the dynamic pressure measured in the Pazy Wing wind tunnel experiments at Technion.**

in the data are the result of wing vibrations and hysteresis that appeared in the experiment (more pronounced at the three degree angle of attack case) [4]. During the tests, the root angle of attack of the wing was fixed and the airspeed of the tunnel was increased, where temporary stops were made at values of 20 m/s, 30 m/s, 40 m/s, and 50 m/s, which introduced some irregularities as it can be seen in Figure 5. Also, time dependent relaxation of the plastic materials (chassis, foil covering) might play a role here. We deliberately omit (nonlinear) regression curves or other means of smoothing of the data because different approaches could be applied for this task, which would require further discussion.

## B. Static Coupling Results

Simulation results and experimental data are compared for the static coupling test cases with root angles of attack of three, five, and seven degrees in this subsection. The legends in the experimental plots presented in the following contain a letter for the particular affiliation or research group and a number to distinguish between different individual methods (e.g. low- or high-fidelity aerodynamics). The relation between affiliation and results is as listed in Table 2. It must be mentioned that not every research group has provided simulation results for all test cases, i.e. most results are plotted for the five degrees angle of attack test case. Some authors have provided aeroelastic simulation results also for the structural model without skin; however, only the results of the models including the skin are plotted in all following sections to enable consistent and meaningful comparisons.

### *Static Coupling Results and Comparison for Three Degrees Root Angle of Attack*

Results of the static coupling simulations in terms of the displacement of the wingtip in the z direction compared to the experimental data of the Pazy Wing are shown in Figure 6 for three degrees root angle of attack of the wing. For this angle of attack, the maximum tip displacement in the experiment is approximately 27%. A slight offset at zero dynamic pressure in the experimental deformations exists, which is due to small pre-deformations in bending and twist

**Table 2** Letters of the affiliations and research groups used in the captions of the comparison plots. Details about the methods and computational frameworks of the individual research groups are given in Section III.

Affiliation / Research Group	Letter in legends
University of Michigan and Georgia Tech	A-1 (Nonlinear beam theory and strip theory) A-2 (Linear FEM and VLM/DLM) A-3 (Nonlinear beam theory and VLM)
Technion	B-1 (MRM with Nastran FEM) B-2 (MRM with beam model)
Imperial College London	D
DLR	E
NASA	G
Metacomp Technologies Inc.	H
ITA and Embraer	I
Siemens Digital Industries Software	J
SIMULIA and Delft University of Technology	K
ZHAW and ETHZ	L
University of São Paulo and Federal University of Bahia	M
University of São Paulo, USP/DAB-Framework	N

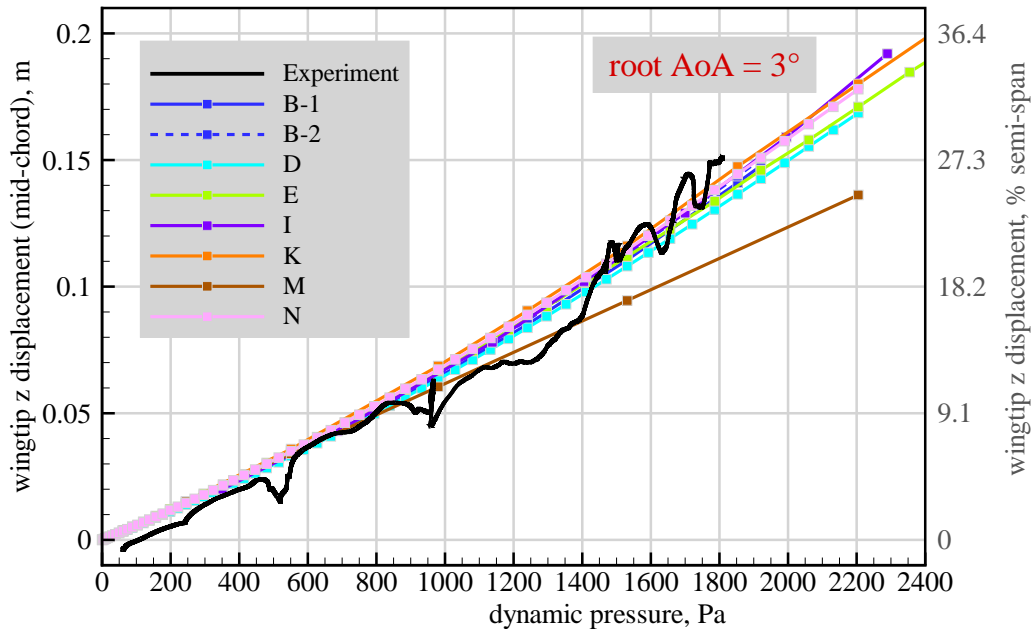


**Fig. 6** Comparison of static coupling results with Pazy Wing experimental data: wingtip displacement in the z direction vs. dynamic pressure for root angle of attack of three degrees. Affiliations/Research Group labeled by upper case letters, cf. Table 2 for the relations.

along the span of the wing even if it is unloaded and possibly due to slight asymmetries that are almost inevitable when manufacturing such a delicate structure. It should be mentioned that the wing was mounted upright in the experiment, which means there is no influence of gravity on the deformation at this root angle of attack. As it can be seen from the simulation results and also from the experimental data, the displacement of the wingtip is a slightly nonlinear function

of the dynamic pressure (the slopes of the curves increase slightly). The agreement between the simulation results of all research groups and the experimental data is very good even for large structural deformations.

*Static Coupling Results and Comparison for Five Degrees Root Angle of Attack*

The comparisons for the five degrees angle of attack are shown in Figure 7. The maximum structural deflection

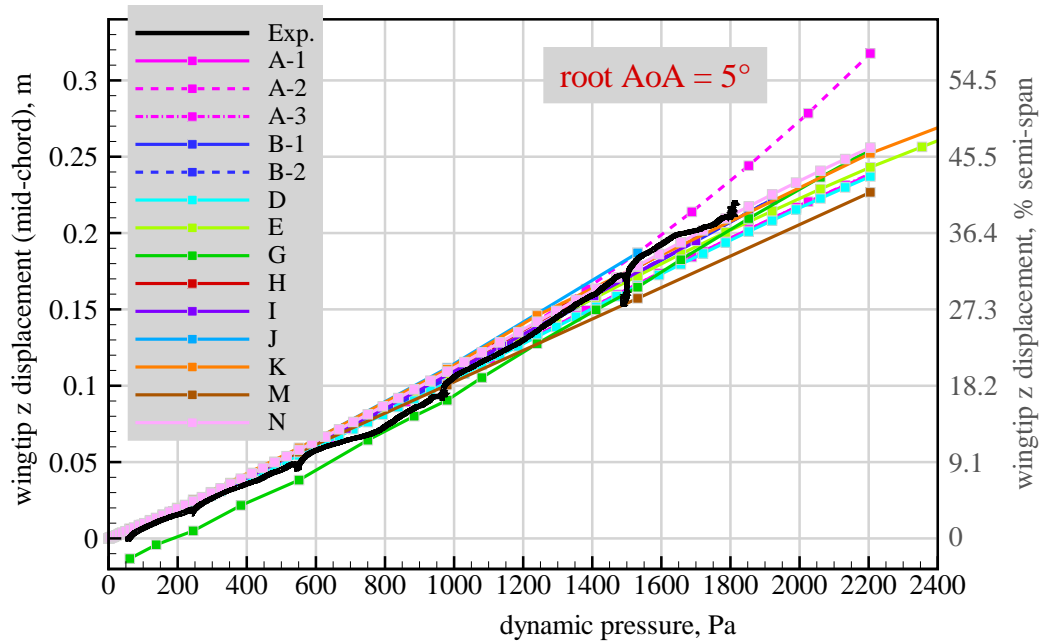


**Fig. 7 Comparison of static coupling results with Pazy Wing experimental data: wingtip displacement in the z direction vs. dynamic pressure for root angle of attack of five degrees.**

reaches approximately 40% for this test case. The slight offset at zero dynamic pressure in the experimental deformations is nonexistent. The slopes of the simulation curves are slightly increasing up to a dynamic pressure of approximately 1300 Pa; beyond that value up to the largest deformations, the slopes reduce. An exception to this is the curve labeled by A-2, for which the slope increases monotonously. The corresponding simulations are based on a FEM-DLM linear model analyzed in MSC Nastran SOL 144, this approach consistently overstates out-of-plane displacements due to an artificial increase of the beam length, which, in turn, further increases the lifting surface areas and thus the aerodynamic forces [49]. In general, a remarkably good agreement between all the simulation results and the experimental data is obtained. Even the largest structural deflections are captured very well. It must be mentioned that the results provided by NASA accidentally did include gravity in the applied forces, which is why they have a negative offset to the rest. The simulation results beyond the maximum dynamic pressure of the experiment (1800 Pa) are close to each other.

*Static Coupling Results and Comparison for Seven Degrees Root Angle of Attack*

The root angle of attack of the third static coupling test case was set to seven degrees. Again, the dynamic pressure was increased from 50 to 1800 Pa in the experiment. Comparisons of the simulation and experimental data are shown in Figure 8. A maximum tip displacement of approximately 50% is obtained in the wind tunnel test. Up to 36% deformation, which is deep in the nonlinear regime, the simulation results closely follow the experimental data. The Pazy Wing tip displacement then deviates from the simulation data, but the overall agreement is very good. The application of a linear method would yield significantly different results, this is demonstrated deliberately by the results from University of Michigan and Georgia Tech (lines labeled by "A-2" in Figures 7 and 8). Not only is the agreement between the simulation results and the experimental data excellent, but the simulation results themselves coincide remarkably well, even though different simulation methods with individual aerodynamic and structural models as well as different computational frameworks were applied.

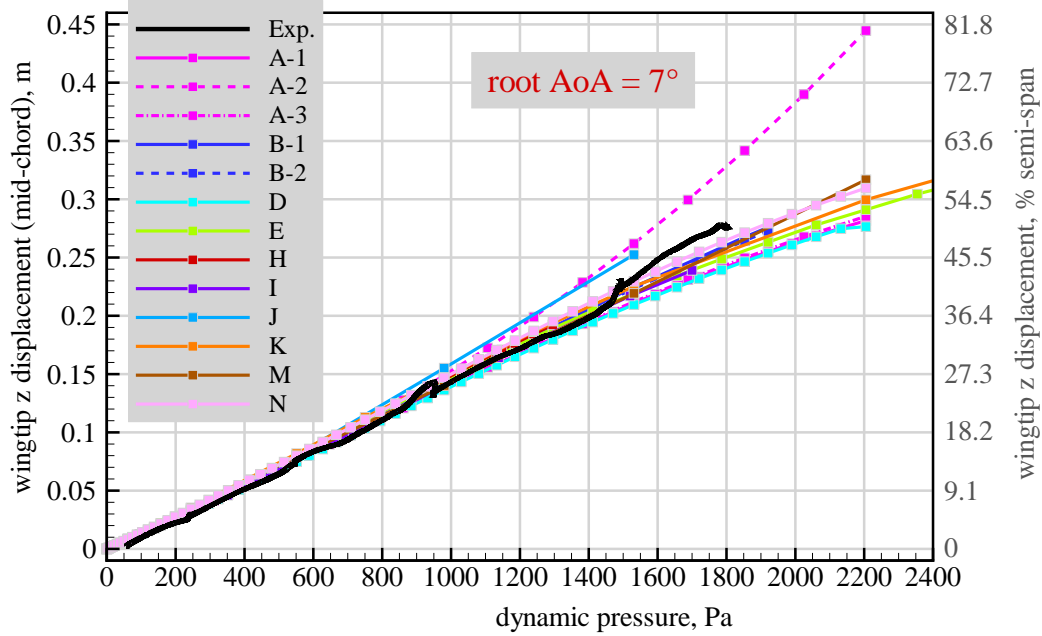


**Fig. 8 Comparison of static coupling results with Pazy Wing experimental data: wingtip displacement in the z direction vs. dynamic pressure for root angle of attack of seven degrees.**

### V. Migration of Eigenvalues as a Function of Static Deformation

Before the comparison of the flutter speeds is presented, the wind-off frequencies of the lowest five structural modes as a function of the static deformation of the wing are investigated and compared. Because the Pazy Wing is an unswept, untapered rectangular wing with an elastic axis close to the mid-chord, the out-of-plane, in-plane, and torsion modes (for the undeformed jig-shape) are clearly distinguishable. If the wing is deformed, geometric couplings between these individual shapes are introduced. For instance, in a state of large out-of-plane deflection, the application of a force in the in-plane (flow) direction introduces a torsional deformation of the wing. To give an impression of the mode shapes about a steady state of large structural deformations, the lowest five structural modes interpolated onto a DLM grid are plotted in Figure 9 together with the static deflection. This was done for a root angle of attack of five degrees and two airspeeds, 1 m/s and 50 m/s, respectively. As it can be seen from the plots, clearly classifiable modes

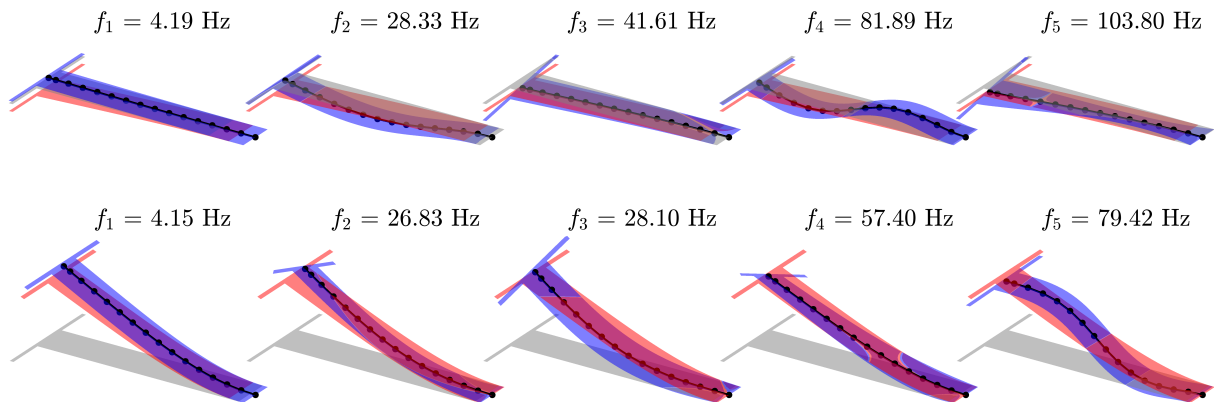


**Fig. 9 The lowest five structural modes interpolated onto a DLM grid for five degrees root angle of attack. Top row corresponds to 1 m/s airspeed, bottom row to 50 m/s. The red surface is the static aeroelastic shape, the blue surface includes the modal deformation.**

are only available for small elastic deformations. For the large deformation case, only modes one and five are distinct out-of-plane bending modes, whereas modes two, three, and four each include a particular amount of torsion.

The computation of the modal frequencies about a pre-loaded state of (large) deflection requires a nonlinear structural formulation. Most approaches for this purpose are based on an eigenvalue analyses of the system which uses the tangential stiffness matrix [35, 50]. Again, the accurate computation of the flutter speed about a state of large steady deflection must capture the changes of the structure's modal characteristics. Unfortunately, there is no experimental data for comparison, and hence the results of the authors are compared with each other.

The frequencies of the five lowest structural modes as a function of the static deformation of the wing (without unsteady aerodynamic forces) are plotted in Figure 10. It is obvious that the nonlinearities have a substantial impact on

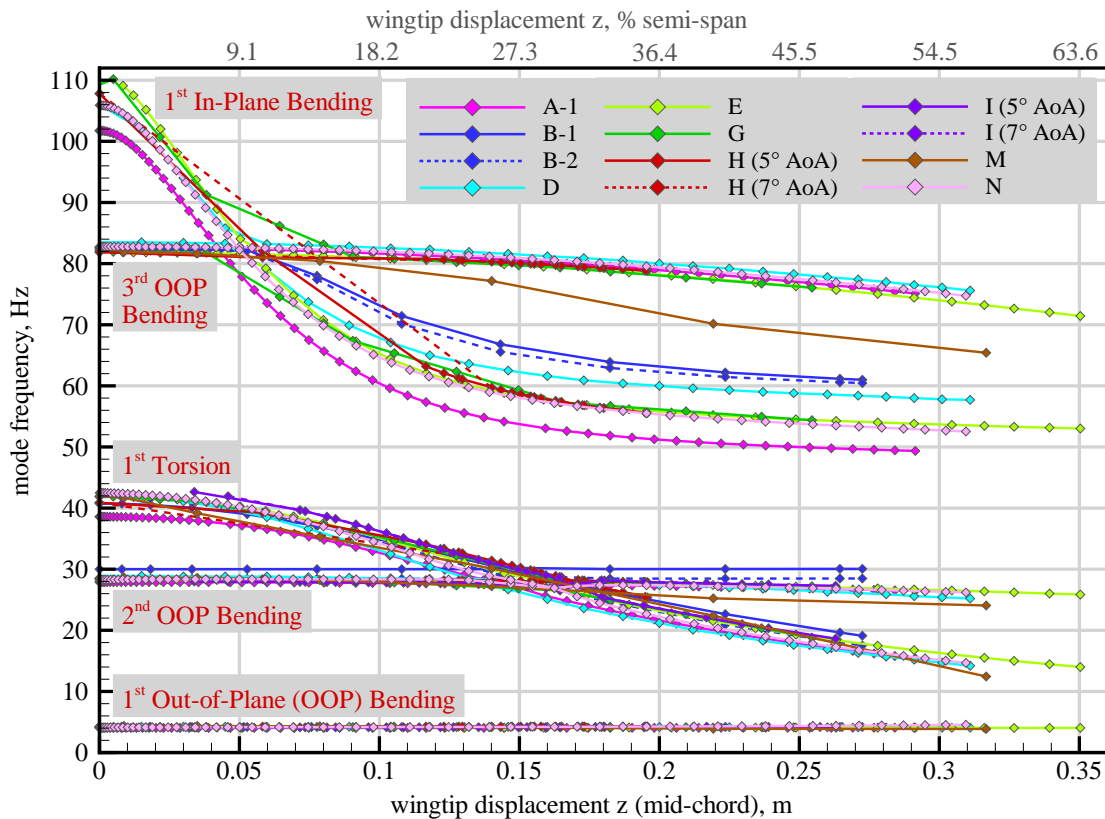


**Fig. 10** Wind-off frequencies of the five lowest structural modes as a function of the static deformation of the Pazy Wing. First torsion and first in-plane bending frequencies drop significantly with increasing level of deformation.

the natural frequencies. Only the first bending mode is marginally affected, despite its great participation in the overall displacement field. In general, the out-of-plane bending modes are much less affected by the structural deformation than the first torsion and the first in-plane bending modes. The latter happens due to the coupling mechanisms mentioned earlier. Most affected are the first torsion and the first in-plane bending modes, as their natural frequencies migrate strongest with increasing deformation (the first in-plane bending mode is reduced in frequency from approximately 110 Hz at zero deformation to approximately 80 Hz at only 10% of structural deformation with respect to semi-span). Another remarkable fact is the coupling or crossing of modes at particular structural deformations. This happens for the first in-plane bending and the third out-of-plane bending mode at approximately 0.06 m / 10% tip displacement. The second out-of-plane bending and the first torsion mode cross at approximately 0.16 m / 29% tip displacement. The crossing of these mode is what drives the hump mode, which is the first flutter region of the Pazy Wing, as will be detailed in the following section.

As for the static coupling test cases, the results of all authors are close together. The nonlinearities, i.e. the migration of the eigenvalues as a function of the deformation, are captured by each individual result. Quantitative differences exist to some extent, however. Most notably for the first in-plane bending mode, where larger differences already exist

at zero displacement of the wing, i.e. in its jig-shape. Also, for larger displacements the computed frequencies of this mode disperse noticeably. Some modes are tracked differently, especially at the crossing of the first in-plane bending and the third out-of-plane bending mode, as can be seen in Figure 10. The static deflection of the wing about which the structure is linearized – i.e., the computation of the pre-loaded eigenvalues and eigenvectors – is obtained by a particular combination of the root angle of attack of the wing and the dynamic pressure. Because nonlinear effects on the aerodynamics are not taken into account, the migration of the frequencies is almost independent of the individual combination of root angle of attack and dynamic pressure. As a consequence of this, the absolute tip displacement can be taken as the independent variable for the plot (as is done on the abscissa).

## VI. Flutter Speed Predictions and Comparison to Experimental Data

The third and final task of the LDWG was the computation of the flutter speeds of the Pazy Wing for the same three root angles of attack. Due to the high flexibility of the model, its flutter characteristics are much more complex than for conventional, i.e., stiffer wings. The flutter speeds depend on the static structural deformation of the wing and thus an additional dimension is introduced in the flutter calculations. It was explained in Section I that at least two nonlinear physical mechanisms play an important role here. First, the aerodynamic forces are tilted towards the wing root as the wing is deflected (they are nonconservative). Second, the structural modal characteristics (eigenvectors, i.e. mode shapes, and eigenvalues) also depend on the structural deflection, as was highlighted in Section V. The migration of the eigenvalues and the changes of the modal characteristics of the wing as a function of the (static) displacement finally impacts the flutter characteristics. In particular, the first flutter mode is a hump mode that "moves" from higher to lower airspeeds as the static deformation of the wing increases. This mechanism was identified already at the beginning of the activities of the LDWG and is described in several publications [11, 14].

Figure 11 depicts the first and the second flutter regions as function of the airspeed and two steady root angles of attack (one degree and five degrees). As it can be seen from this plot the hump mode, which is formed by the second

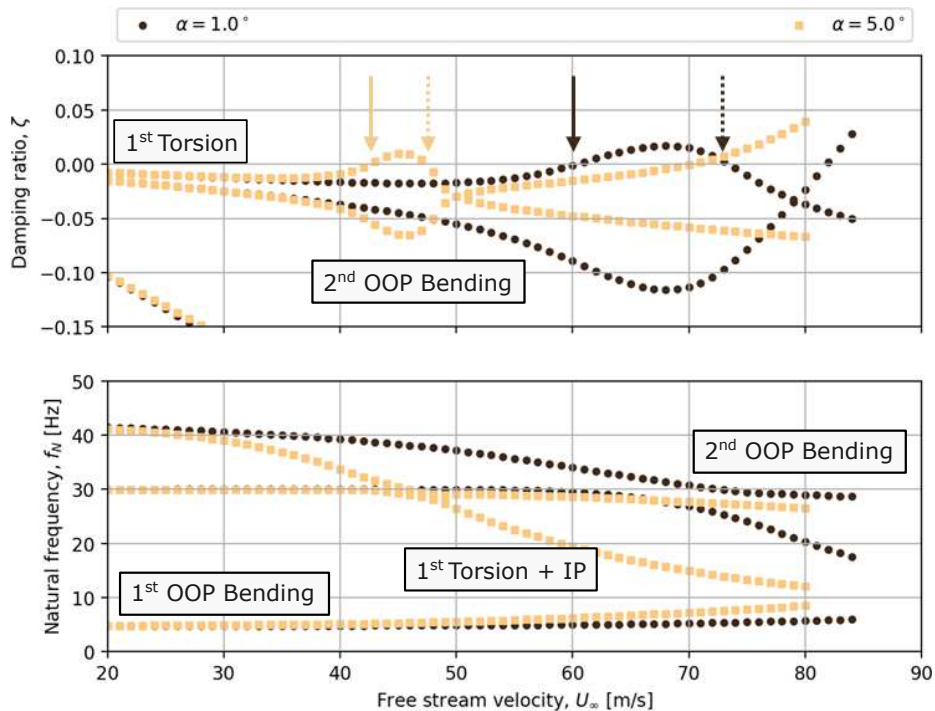


**Fig. 11** Exemplary frequency and damping diagrams of the Pazy Wing as a function of airspeed and two root angles of attack. First flutter instability at five degrees angle of attack: 43 m/s, 1<sup>st</sup> torsion + 2<sup>nd</sup> OOP bending (hump mode). Second instability at five degrees angle of attack: 71 m/s, 1<sup>st</sup> torsion + 2<sup>nd</sup> OOP bending. The hump mode moves to lower airspeeds with increasing deformation, on and offset speeds are marked by solid and dashed arrows, respectively.



out-of-plane bending and the first torsion mode, crosses the zero damping line at approximately 60 m/s for the root angle of attack of one degree, and at approximately 43 m/s for five degrees angle of attack. Its offset speed is reduced even more with increasing deformation, thus the hump mode appears steeper with increasing steady deformation<sup>||</sup>. The second flutter instability (formed by the first torsion and the first out-of-plane bending modes) appears at a much higher airspeed (above 70 m/s), additionally, the damping curve crosses the line of zero damping with a much stronger gradient. For the hump mode both a flutter onset and an offset speed can be calculated. In the wind tunnel experiment, the root angle of attack of the wing was fixed and the airspeed was increased gradually. Regions of aeroelastic instability had been entered (flutter onset speed), but the oscillation amplitudes were limited due to nonlinearities that led to limit cycle oscillations (LCO), and once the airspeed was increased further, the oscillations of the wing settled down (flutter offset speed). This approach can only be conducted safely if the flutter mechanism is of the "soft" type and a supercritical bifurcation (LCO) is entered in which the amplitude is limited reliably by particular nonlinear effects (mostly aerodynamic stall because of boundary layer separation due to strong adverse pressure gradients).

Most of the authors first calculated the static equilibrium (static coupling) of the wing for a combination of steady root angle of attack and airspeed and then linearized the system (both the aerodynamic and the structural part). Depending on the implementation, a frequency-domain flutter calculation (e.g.  $p - k$  method) or an eigenvalue analysis of a linearized state-space formulation ( $p$  method) can be used to find the regions of instability. Also time-domain methods were used, a 3D source and doublet panel method and a CFD-based approach, cf. the description in Section III. The simulation results of the authors in terms of the flutter onset and offset speeds are shown together with the experimental data in Figure 12. As for the static coupling simulations, the comparisons reveal a remarkably good agreement between

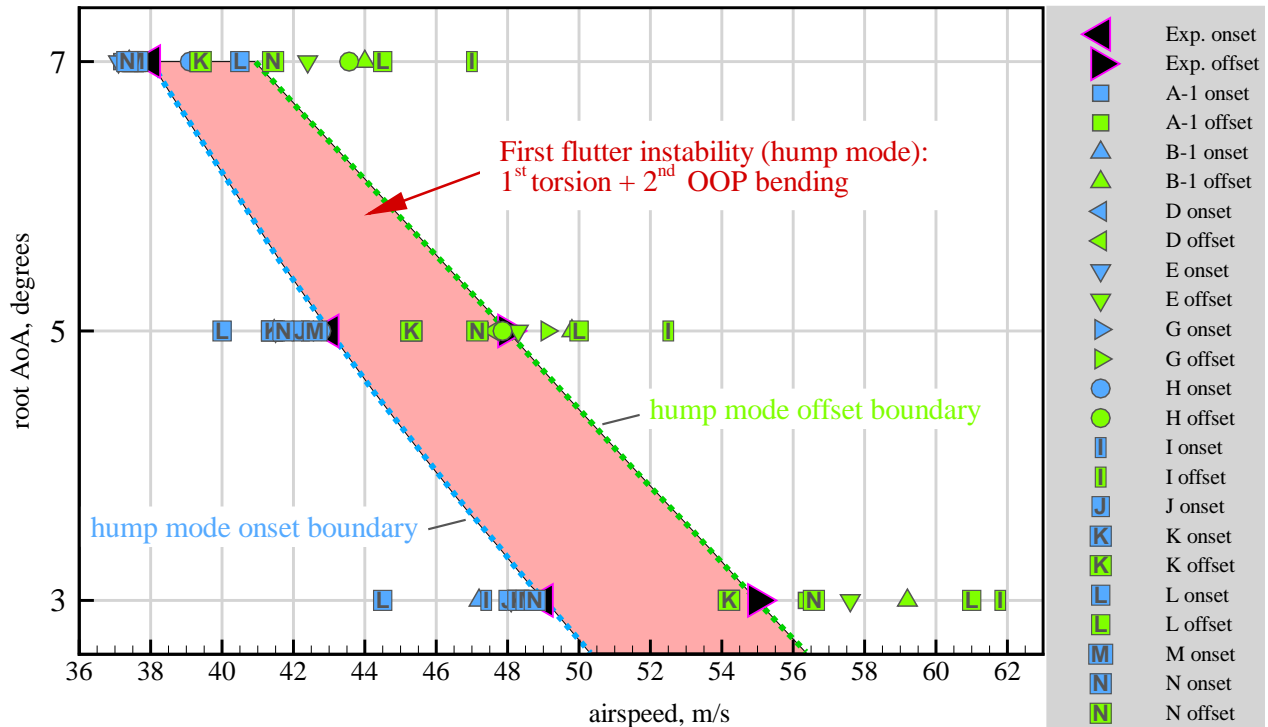


**Fig. 12** Pazy Wing flutter on and offset speeds from simulations and experiment as a function of the root angle of attack. Note that no experimental data point exists for the offset speed at seven degrees angle of attack. On and offset boundaries of the hump mode are interpolated between experimental data points (offset speed at seven degrees angle of attack is taken from computation [5]). Figure 14 provides individual plots.

the hump mode flutter on and offset speeds from the wind tunnel experiment and the simulations, especially when the zoomed speed range of the plot, which ranges from 36 m/s to 63 m/s, is considered. This result is also remarkable given the fact that different methods are used for the aerodynamic (strip theory, linearized UVLM, DLM, 3D source

<sup>||</sup>This behavior must be considered for the simulation of limit cycle oscillations, which is a topic of current research [13]. For time-domain simulations, the aeroelastic damping can become very low in magnitude such that amplitudes increase only marginally over time [9, 13, 15].

and doublet panel method, CFD/Navier-Stokes) and the structural disciplines (full FEM, beam model with nonlinear beam theories, beam model with commercial programs). With the exception of the CFD-based simulation program, viscous effects are not considered by the individual computational frameworks of the research groups. As is typical for aeroelastic systems in the regime of low speed and attached flow, viscous effects only play a secondary role. Their main contribution is the (steady) thickening of the boundary layer on the suction side of the wing, which introduces the well-known viscous decambering effect [32], but the unsteady aerodynamic characteristics (as represented e.g. by Theodorsen's function) are mostly unaffected. Because the plot in Figure 12 appears filled and some symbols are hidden, all simulation results are shown in an individual plot together with the experimental data in the Appendix IX.

This conclusion is confirmed by a comparison of the mean values and standard deviations (of the data from Figure 12) of the calculated flutter on and offset speeds with the experimental data, plotted in Figure 13. The experimental

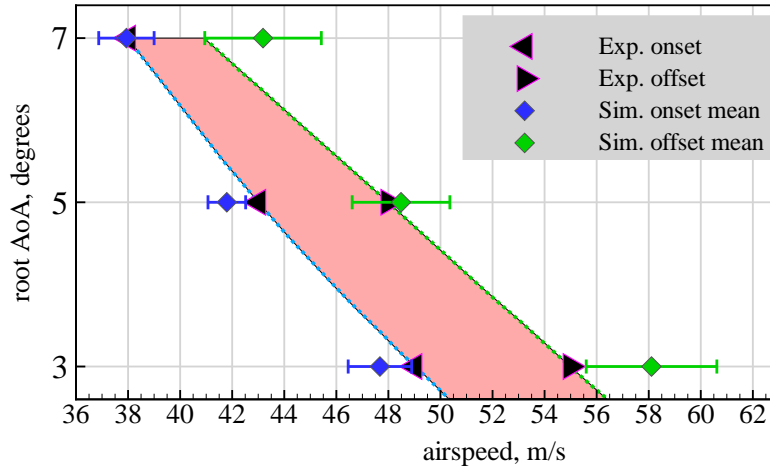


**Fig. 13 Means and standard deviations of all computed flutter on and offset speeds (from data in Figure 12).**

and simulated flutter onset speed for the seven degrees root angle of attack case are almost identical. Also for the five degrees root angle of attack case, the agreement is excellent. Differences are slightly increased for the offset speed of the three degrees root angle of attack case. Standard deviations are larger for the flutter offset speeds than for the onset speeds. The corresponding numerical data of these results are listed in Table 3. The maximum difference of 6.2% appears for the flutter offset speeds for the three degrees angle of attack case.

**Table 3 Mean values and standard deviations (from data in Figure 13) of flutter on and offset speeds from all simulations; quantitative comparison of mean values from simulations to experimental data.**

Angle of attack	degrees	3	5	7
Flutter onset speed experiment	m/s	49	43	38
Mean flutter onset speed simulations	m/s	47.7	41.8	37.9
Standard deviation flutter onset speed simulations	m/s	1.2	0.7	1.1
$\Delta$ onset speeds, $\left  \frac{sim-exp}{exp} \right $	%	2.7	2.8	0.3
Flutter offset speed experiment	m/s	55	48	-
Mean flutter offset speed simulations	m/s	58.4	48.6	43.5
Standard deviation flutter offset speed simulations	m/s	2.5	1.9	2.2
$\Delta$ offset speeds, $\left  \frac{sim-exp}{exp} \right $	%	6.2	1.3	-

## VII. Conclusion and Outlook

In this work, results of the Large Deflection Working Group of the Third Aeroelastic Prediction Workshop are presented. The test case is the Pazy Wing from Technion - Israel Institute of Technology, a highly flexible wind tunnel benchmark model which shows elastic structural deflections up to 50% with respect to the semi-span, but is simple in its setup (unswept, untapered, rectangular wing). Hence an aeroelastic simulation model of the wing can be setup easily. Three kinds of simulations were conducted by the research groups. First, static coupling for three different root angles of attack (three degrees, five degrees, and seven degrees). Second, the computation of the natural vibration characteristics (mode shape frequencies) about the statically deformed structure. Third, the computation of the on and offset speeds of the first flutter instability (a hump mode), also for three different root angles of attack. Different aeroelastic computational frameworks with different aerodynamic and structural methods have been used by the authors, ranging from strip theory, VLM, UVLM, DLM, 3D source and doublet panel method, to a CFD-based approach.

All static coupling results (wingtip displacements) for three, five, and seven degrees root angle of attack are remarkably close to the experimental data. The results for the migration of the structural eigenvalues as a function of the tip displacement of the wing are in good agreement, which demonstrates that all frameworks are capable of capturing the relevant nonlinearities. Also the results of the flutter simulations (on and offset speeds of the first flutter region, a hump mode) are in good agreement with the corresponding data from the experiment. It can be concluded that the computational methods and frameworks which were applied by the authors all capture the decisive nonlinear aeroelastic effects: rotation of the aerodynamic forces (non conservative in nature) as the deformation of the wing is increased, and the dependence of the modal structural properties (eigenvectors and eigenvalues) on the static deformation.

Although simple in its setup, the Pazy Wing test case offers wide possibilities for future research. An interesting feature is that, depending on the level of detail the investigation aims to consider, a variety of approximations of the aerodynamic and the structural system can be made where each approximation yields insight into a particular aerodynamic and structural effect. For instance, the layout of the wing, which is composed of the aluminum spar, the 3D printed Nylon chassis, and the foil covering can be modeled by a simple (but nonlinear) finite element beam, but it can also be considered and modeled as a much more complex structural part. The foil covering (a polyester shrink film with heat activated adhesive on one side), which is applied onto the chassis by an iron and a heat gun, provides a smooth and clean surface, but this process inevitably introduces a pre-tension of the foil (which is of course desired). This pre-tension and the specific shape of the corresponding shell or membrane elements (of the foil in the full FEM) is difficult to estimate and to model. It introduces certain nonlinear effects (e.g. wrinkling of the foil at the side which is compressed in bending depending on the intensity of the pre-tension) that have not been considered and analyzed extensively in an aeroelastic context (furthermore, this effect impacts the aerodynamics of the wing at a very local level in a nonlinear fashion). That conclusion analogously holds for the aerodynamics. Simulation models of different accuracy can be applied depending on the availability and the objective of the analysis: A high-fidelity CFD method with free transition modeling based on a computational grid or geometry that includes the true outer surface of the wing (i.e., the sagging between the ribs, as highlighted in Figure 3) gives insight into complex flow structures such as laminar separation bubbles with different shapes and locations on the wing depending on the root angle of attack.

## VIII. Acknowledgments

The support of all the members of the Large Deflection Working Group and of the AePW3 is appreciated. The authors are grateful to Technion for making the models and experimental data of the Pazy Wing freely available to the community. Also the support of the DLR Institute of Aeroelasticity for this work is acknowledged.

## IX. Appendix: Individual Flutter Results and Comparisons with Experimental Data

Because the plot in Figure 12 appears filled and some symbols are hidden, all simulation results are shown in an individual plot together with the experimental data in Figure 14.

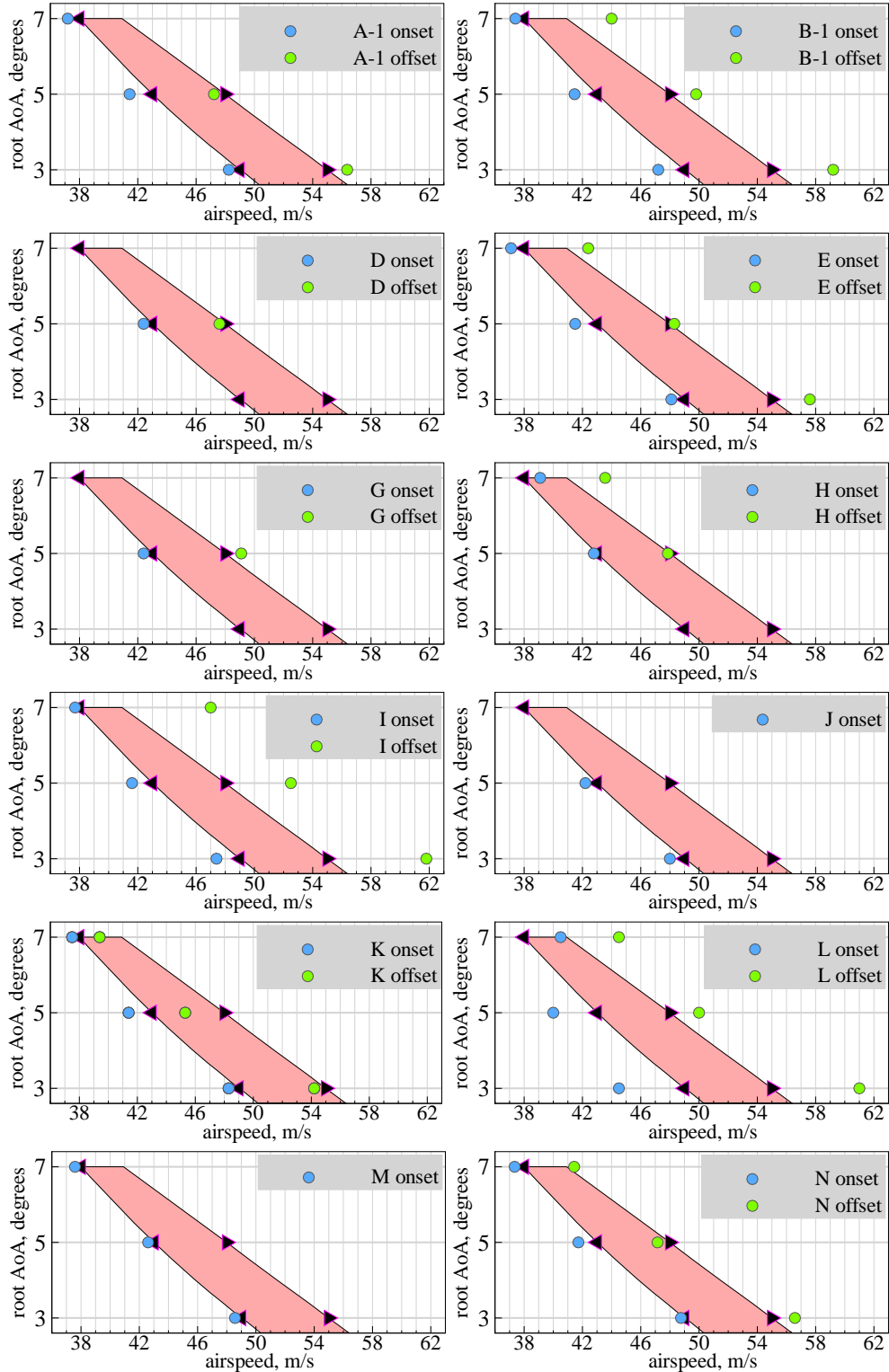


**Fig. 14 Pazy Wing flutter on and offset speeds – individual results and comparisons with experimental data. Note that no experimental data point exists for the offset speed at seven degrees angle of attack.**

## References

- [1] Tang, D. and Dowell, E. H., “Experimental and Theoretical Study on Aeroelastic Response of High-Aspect-Ratio Wings,” *AIAA Journal*, Vol. 39, No. 8, 2001, pp. 1430–1441.
- [2] Cesnik, C. E. S., Senatore, P. J., Su, W., Atkins, E. M., and Shearer, C. M., “X-HALE: A Very Flexible Unmanned Aerial Vehicle for Nonlinear Aeroelastic Tests,” *AIAA Journal*, Vol. 50, No. 12, 2012, pp. 2820–2833.
- [3] Ritter, M., Dillinger, J., and Meddaikar, Y. M., “Static and Dynamic Aeroelastic Validation of a Flexible Forward Swept Composite Wing,” 58<sup>th</sup> AIAA/ASCE/AHS/ASC Structures, Structural Dynamics, and Materials Conference, Grapevine, Texas, Jan 2017.
- [4] Avin, O., Raveh, D. E., Drachinsky, A., Ben-Shmuel, Y., and Tur, M., “Experimental Aeroelastic Benchmark of a Very Flexible Wing,” *AIAA Journal*, Vol. 60, No. 3, 2022, pp. 1745–1768.
- [5] Drachinsky, A. and Raveh, D. E., “Nonlinear Aeroelastic Analysis of Highly Flexible Wings using the Modal Rotation Method,” *AIAA Journal*, Vol. 60, No. 5, 2022, pp. 3122–3134.
- [6] Drachinsky, A., Avin, O., Raveh, D. E., Ben-Shmuel, Y., and Tur, M., “Flutter Tests of the Pazy Wing,” *AIAA Journal*, Vol. 60, No. 9, 2022, pp. 5414–5421.
- [7] Drachinsky, A., Freydin, M., and Raveh, D. E., “Large Deformation Shape Sensing Using a Nonlinear Strain to Displacement Method,” *AIAA Journal*, Vol. 60, No. 9, 2022, pp. 5547–5558.
- [8] Riso, C. and Cesnik, C. E. S., “Impact of Low-Order Modeling on Aeroelastic Predictions for Very Flexible Wings,” *Journal of Aircraft*, Vol. 60, No. 3, 2023, pp. 662–687.
- [9] Riso, C. and Cesnik, C. E. S., “Geometrically Nonlinear Effects in Wing Aeroelastic Dynamics at Large Deflections,” *Journal of Fluids and Structures*, Vol. 120, 2023.
- [10] Maraniello, S. and Palacios, R., “State-Space Realizations and Internal Balancing in Potential-Flow Aerodynamics with Arbitrary Kinematics,” *AIAA Journal*, Vol. 57, No. 6, 2019, pp. 2308–2321.
- [11] Goizueta, N., Drachinsky, A., Wynn, A., Raveh, D., and Palacios, R., “Flutter Predictions for Very Flexible Wing Wind Tunnel Test,” *AIAA Scitech 2021 Forum*, Virtual Conference, Jan 2021.
- [12] Righi, M., “Uncertainties Quantification in Flutter Prediction of a Wind Tunnel Model Exhibiting Large Displacements,” *AIAA Scitech 2021 Forum*, Virtual Conference, Jan 2021.
- [13] Righi, M., “Uncertainties Quantification in the Prediction of the Aeroelastic Response of The Pazy Wing Tunnel Model,” *AIAA Scitech 2023 Forum*, National Harbor, Maryland, Jan 2023.
- [14] Hilger, J. and Ritter, M. R., “Nonlinear Aeroelastic Simulations and Stability Analysis of the Pazy Wing Aeroelastic Benchmark,” *Aerospace*, Vol. 8, No. 10, 2021.
- [15] Ritter, M. and Hilger, J., “Dynamic Aeroelastic Simulations of the Pazy Wing by UVLM with Nonlinear Viscous Corrections,” *AIAA Scitech 2022 Forum*, Virtual Conference, Jan 2022.
- [16] Ritter, M., Fehrs, M., and Mertens, C., “Aerodynamic and Static Coupling Simulations of the Pazy Wing with Transitional CFD for the Third Aeroelastic Prediction Workshop,” *AIAA Scitech 2023 Forum*, National Harbor, Maryland, Jan 2023.
- [17] Stanford, B., Jacobson, K., and Chwalowski, P., “Aeroelastic Analysis of Highly Flexible Wings with Linearized Frequency-Domain Aerodynamics,” *accepted by Journal of Aircraft, to be published*.
- [18] Melo, F. B. C., Bussamra, F. L. S., and Verri, A. A., “Methodology to Assess the Effects of Geometric Nonlinearity on the Static Aeroelastic Behavior of Very Flexible Wings,” *International Forum on Aeroelasticity and Structural Dynamics IFASD*, Madrid, Spain, June 2022.
- [19] Lima, J. F. B. O., Bussamra, F. L. S., Verri, A. A., and Melo, F. B. C., “Methodology to Evaluate Flutter on Geometric Nonlinear Structural Wings Applied to the PazyWing,” *AIAA SciTech Forum 2024, to be published*.
- [20] Ribeiro, A. F. P., Casalino, D., and Ferreira, C., “Free Wake Panel Method Simulations of a Highly Flexible Wing at Flutter,” *2022 AIAA Aviation and Aeronautics Forum*, Chicago, Illinois, 2022.
- [21] Ribeiro, A. F., Casalino, D., and Ferreira, C., “Free Wake Panel Method Simulations of a Highly Flexible Wing in Flutter and Gusts,” *Journal of Fluids and Structures*, Vol. 121, 2023.

- [22] Fehrs, M., Ritter, M., Helm, S., and Mertens, C., “CFD simulations of the Pazy Wing in Support of the Third Aeroelastic Prediction Workshop,” *International Forum on Aeroelasticity and Structural Dynamics IFASD*, Madrid, Spain, June 2022.
- [23] Su, W. and Cesnik, C. E. S., “Nonlinear Aeroelasticity of a Very Flexible Blended-Wing-Body Aircraft,” *Journal of Aircraft*, Vol. 47, No. 5, Sep 2010, pp. 1539–1553.
- [24] Su, W. and Cesnik, C. E. S., “Strain-Based Geometrically Nonlinear Beam Formulation for Modeling Very Flexible Aircraft,” *International Journal of Solids and Structures*, Vol. 48, No. 16–17, 2011, pp. 2349–2360.
- [25] Cesnik, C. E. S. and Hodges, D. H., “VABS: A New Concept for Composite Rotor Blade Cross-Sectional Modeling,” *Journal of the American Helicopter Society*, Vol. 42, No. 1, 1997, pp. 27–38.
- [26] Riso, C., Sanghi, D., Cesnik, C. E. S., Vetrano, F., and Teufel, P., “Parametric Roll Maneuverability Analysis of a High-Aspect-Ratio-Wing Civil Transport Aircraft,” *AIAA SciTech 2020 Forum*, Orlando, FL, Jan 2020.
- [27] Peters, D. A., Hsieh, M. C. A., and Torrero, A., “A State-Space Airloads Theory for Flexible Airfoils,” *Journal of the American Helicopter Society*, Vol. 52, No. 4, 2007, pp. 329–342.
- [28] Drachinsky, A. and Raveh, D. E., “Modal Rotations: A Modal-Based Method for Large Structural Deformations of Slender Bodies,” *AIAA Journal*, Vol. 58, No. 7, 2020, pp. 3159–3173.
- [29] del Carre, A., Muñoz-Simón, A., Goizueta, N., and Palacios, R., “SHARPy: A dynamic aeroelastic simulation toolbox for very flexible aircraft and wind turbines,” *Journal of Open Source Software*, Vol. 4, No. 44, Dec. 2019.
- [30] Goizueta, N., Wynn, A., and Palacios, R., “Adaptive Sampling for Interpolation of Reduced-Order Aeroelastic Systems,” *AIAA Journal*, Vol. 60, No. 11, 2022, pp. 6183–6202.
- [31] Katz, J. and Plotkin, A., *Low-Speed Aerodynamics*, Cambridge Aerospace Series, Cambridge University Press, 2001.
- [32] Drela, M., *Flight Vehicle Aerodynamics*, MIT Press, 2014.
- [33] Ritter, M., Jones, J., and Cesnik, C. E. S., “Free-flight Nonlinear Aeroelastic Simulations of the X-HALE UAV by an Extended Modal Approach,” *International Forum on Aeroelasticity and Structural Dynamics IFASD*, Como, Italy, 2017.
- [34] Drela, M., *XFOIL: An Analysis and Design System for Low Reynolds Number Airfoils*, Springer Berlin Heidelberg, 1989, pp. 1–12.
- [35] MSC, *MSC Nastran 2017 Nonlinear User’s Guide SOL 400*, MacNeal-Schwendler Corporation, 2014.
- [36] Ritter, M., Hilger, J., and Zimmer, M., “Static and Dynamic Simulations of the Pazy Wing Aeroelastic Benchmark by Nonlinear Potential Aerodynamics and detailed FE Model,” *AIAA Scitech 2021 Forum*, Virtual Conference, Jan 2021.
- [37] Verri, A. A., Jorge, C. T., Bizarro, A. F., Bussamra, F. L. S., Júnior, H. N. S., and Cesnik, C. E. S., “Multidisciplinary Methods for Wing Flight Shape Analysis—Effect of the Geometric Nonlinear Structure for Static Pull-up,” *31st Congress of the International Council of the Aeronautical Sciences—ICAS*, 2018.
- [38] Lima, J. F. B. O., *Methodology to Evaluate Flutter on Geometric Nonlinear Structural Wings Applied to the Pazy Wing*, Master’s thesis, São José dos Campos, 2023.
- [39] Zhao, W., Kapania, R. K., Schetz, J. A., and Coggin, J. M., “Nonlinear Aeroelastic Analysis of SUGAR Truss-braced Wing (TBW) Wind-tunnel Model (WTM) under in-plane Loads,” *56th AIAA/ASCE/AHS/ASC Structures, Structural Dynamics, and Materials Conference*, Kissimmee, Florida, Jan 2015.
- [40] Xie, C., Liu, Y., Yang, C., and Cooper, J. E., “Geometrically Nonlinear Aeroelastic Stability Analysis and Wind Tunnel Test Validation of a Very Flexible Wing,” *Shock and Vibration*, Vol. 2016, 2016.
- [41] Siemens, *Simcenter Nastran 2020.1 Quick Reference Guide*, Siemens AG, 2020.
- [42] Reddy, J. N., *An Introduction to Nonlinear Finite Element Analysis Second Edition: With Applications to Heat Transfer, Fluid Mechanics, and Solid Mechanics*, OUP Oxford, 2014.
- [43] Zienkiewicz, O. and Taylor, R., *The Finite Element Method for Solid and Structural Mechanics*, Elsevier Science, 2005.
- [44] Benini, G., Belo, E., and Marques, F., “Numerical model for the simulation of fixed wings aeroelastic response,” *Journal of the Brazilian Society of Mechanical Sciences and Engineering*, Vol. 26, 2004, pp. 129–136.

- [45] Guillaume, P., Verboven, P., Vanlanduit, S., Van der Auweraer, H., and Peeters, B., “A Poly-Reference Implementation of the Least-Squares Complex Frequency-Domain Estimator,” *Proceedings of IMAC*, 2003.
- [46] dos Santos, J. P. T. P., *Nonlinear Aeroelastic Simulation of Flexible Wings*, Master’s thesis, Escola de Engenharia de São Carlos da Universidade de São Paulo (EESC-USP), 2023.
- [47] dos Santos, J. T. P., Beghini, G. R., and Marques, F. D., “Time Domain Aeroelastic Analysis of the Pre-Pazy and Pazy Wings,” XIX International Symposium on Dynamic Problems of Mechanics (DINAME 2023), Brazilian Association of Engineering and Mechanical Sciences – ABCM, 2023.
- [48] Riso, C. and Cesnik, C. E., *Correlations Between UM/NAST Nonlinear Aeroelastic Simulations and the Pre-Pazy Wing Experiment*, AIAA Scitech 2021 Forum, Virtual Conference, Jan 2021.
- [49] Ritter, M. R., *An Extended Modal Approach for Nonlinear Aeroelastic Simulations of Highly Flexible Aircraft Structures*, Dissertation, Technische Universität Berlin, 2019.
- [50] Bathe, K. J., *Finite Element Procedures*, Prentice Hall, Pearson Education, Inc., 2006.